Neural Cell Adhesion Molecule-Deficient β-Cell Tumorigenesis Results in Diminished Extracellular Matrix Molecule Expression and Tumour Cell-Matrix Adhesion

Joakim Håkansson[a]   Xiaojie Xian[a]   Liqun He[a]   Anders Ståhlberg[b]
Sven Nelander[a]   Tore Samuelsson[a]   Mikael Kubista[b]   Henrik Semb[a]

[a]Department of Medical Biochemistry, Göteborg University, and [b]TATAA Biocenter, Göteborg, Sweden

Abstract

To understand by which mechanism neural cell adhesion molecule (N-CAM) limits β tumour cell disaggregation and dissemination, we searched for potential downstream genes of N-CAM during β tumour cell progression by gene expression profiling. Here, we show that N-CAM-deficient β-cell tumorigenesis is associated with changes in the expression of genes involved in cell-matrix adhesion and cytoskeletal dynamics, biological processes known to affect the invasive and metastatic behaviour of tumour cells. The extracellular matrix (ECM) molecules emerged as the primary target, i.e. N-CAM deficiency resulted in down-regulated mRNA expression of a broad range of ECM molecules. Consistent with this result, deficient deposition of major ECM stromal components, such as fibronectin, laminin 1 and collagen IV, was observed. Moreover, N-CAM-deficient tumour cells displayed defective matrix adhesion. These results offer a potential mechanism for tumour cell disaggregation during N-CAM-deficient β tumour cell progression. Prospective consequences of these findings for the role of N-CAM in β tumour cell dissemination are discussed.

Copyright © 2005 S. Karger AG, Basel

J.H. and X.X. contributed equally to this paper.

Introduction

During development of human cancer, neural cell adhesion molecule (N-CAM) expression undergoes significant changes. In colon carcinoma, pancreatic cancer and astrocytoma, N-CAM expression is markedly down-regulated, and this loss of N-CAM correlates with poor prognosis [1]. Moreover, in various cancer types, expression of N-CAM shifts from the adult 120-kDa isoform to the embryonic 140- and 180-kDa isoforms, together with a general down-regulation of expression [1]. The biological significance of this change in N-CAM expression and its role in tumour onset and/or progression are, however, not understood.

To study the functional role of N-CAM in tumour development, we have used the transgenic Rip1Tag2 (RT) multistage mouse tumour model that develops β-cell-specific tumours in the pancreatic islets of Langer-

Dr. Henrik Semb
Section of Endocrinology, Stem Cell Centre
Lund University, BMC, B10, Klinikgatan 26
SE–22184 Lund (Sweden)
Tel. +46 46 2223159, Fax +46 46 2223600, E-Mail Henrik.Semb@endo.mas.lu.se

hans as a consequence of the expression of SV40 large T antigen under the control of the rat insulin 1 promoter [2]. RT tumour progression involves hyperplasia, angiogenesis, adenoma and carcinoma formation, but not metastasis. The latter may be explained by the fact that the mice succumb to hypoglycaemia prior to the time it takes for metastasis to develop in the RT model. Recently, we showed that N-CAM limits tumour cell dissemination during tumour progression in the RT tumour model [3]. N-CAM is a member of the immunoglobulin superfamily of CAMs, mediating Ca^{2+}-independent homotypic and heterotypic cell-cell adhesion through homophilic and heterophilic binding mechanisms. Whereas RT tumours normally do not metastasize, approximately 50% of RT mice lacking one or two functional *N-CAM* alleles (RT[NC/KO]) developed metastases mainly to local lymph nodes but also to distant organs, indicating both haematogenous and lymphatic spreading of the tumour cells. Strikingly, re-expression of N-CAM-120 in β tumour cells totally prevented metastasis, indicating that N-CAM within β tumour cells plays a causal role in limiting tumour cell spreading [3]. Histopathological analysis of N-CAM-deficient tumours revealed extensive tissue disaggregation resulting in the appearance of tumour cell clusters in haemorrhagic lacunae, suggesting changes in tumour cell-matrix adhesion [4]. However, the molecular mechanism for N-CAM's inhibitory effect on metastatic β tumour cell spreading in vivo remains unknown.

The aim of this study was to elucidate the mechanism by which N-CAM deficiency causes β tumour cell metastasis. For this purpose, we explored potential downstream components of N-CAM during β cell tumorigenesis by the use of cDNA microarray experiments.

We show that N-CAM deficiency during β cell tumorigenesis resulted in coherent down-regulated expression of extracellular matrix (ECM) molecules, which correlated with deficient deposition of ECM components within the tumour cell stroma, and deficient tumour cell-matrix adhesion. These findings emphasize the significance of N-CAM in cell-matrix adhesion and serve as an informative platform to further unravel by which mechanism N-CAM affects β tumour cell spreading.

Material and Methods

Mice
RT and RT[NC/KO] mice were housed and bred at the Department of Experimental Biochemistry at Göteborg University according to Swedish animal research regulations. N-CAM knock-out mice (with C57/BL6 background) were bred with RT mice to generate RT[NC/KO]

and RT littermates. Glucose (5% weight/volume) was fed to all tumour-bearing mice when they reached 6 weeks of age to compensate the hypoglycaemia induced by the insulinoma.

Islet Preparation and RNA Extraction
Islets of Langerhans were isolated from 8-week-old RT and RT[NC/KO] mice. Total RNA was prepared using the RNeasy mini kit (Qiagen) with the RNase-free DNase (Qiagen) treatment according to the manufacturer's instructions. To avoid individual variation due to the fact that only 50% of RT[NC/KO] mice develop metastasis, RNA from 6 RT and 7 RT[NC/KO] mice, respectively, was pooled.

T7 RNA Amplification of in vivo Material
Two cycles of T7 RNA (aRNA) amplification were performed from 2 µg of total RNA according to a published protocol [5], with the only change that no linear acrylamide was used in the first step.

Microarray Hybridization
The amplified RNA from RT and RT[NC/KO] mice was compared on cDNA microarray chips containing totally 5,501 different genes. The hybridization was repeated 4 times on one chip containing 1,161 genes and 3 times on another chip containing 4,800 genes (some genes were printed on both chips). The fold change was calculated as an average for the hybridizations. Student's t test was used to calculate the p value, and only genes that had $p \leq 0.05$ were used in further analysis.

Scanning and Data Analysis
The chips were scanned (ScanArray 3000, Packard Bioscience, Meriden, Conn., USA), the data processes and statistics analysis performed as previously described [5].

Gene Classification by Gene Ontology
Gene Ontology Annotation uses a controlled vocabulary and facilitates the identification of genes related to a specific biological process, molecular function and cellular component. Celera Gene Ontology Annotation was used to identify these gene groups.

Analyses of the Extent of Gene Expression Changes within Gene Groups
There were 5,501 different genes on the cDNA microarray chips. When using the expression ratio 1.5 and a p value of 0.05 as cut-off for the significant regulation of differentially regulated genes, there were 401 up-regulated genes and 296 down-regulated genes. Thus, the ratio for up-regulated genes was 401/5,501 = 0.073, and the ratio for down-regulated genes was 296/5,501 = 0.054. The high number of regulated genes suggests that some of them may be false positive. To test whether a more stringent cut-off value would change our conclusions, we used a cut-off value of $p \leq 0.01$. Importantly, this did not change the regulated gene groups (table 2, fig. 2). The only difference was that the number of genes in some of the groups decreased. However, all numbers of regulated genes within the ECM group remained the same. Each gene group was classified by Gene Ontology terms. The total number of genes in each group was counted, as well as the up-regulated and down-regulated gene numbers. The regulated gene numbers were compared with the expected regulated gene numbers in the corresponding groups. The expected up-regulated gene number in each group was given by the total gene number in that group × 0.073, and the expected down-regulated gene number in each group was given by the total gene number in that group × 0.054. Then,

Håkansson/Xian/He/Ståhlberg/Nelander/
Samuelsson/Kubista/Semb

Table 1. Primers used for quantitative RT-PCR

| Gene	Primer	Sequence
Acidic ribosomal phosphoprotein PO	Forward Reverse	5′-CGACCTGGAAGTCCAACTAC-3′ 5′-ATC TGC TGC ATC TGC TTG-3′
β-Tubulin, chain 5	Forward Reverse	5′-CCTTCATTGGAAACAGCACA-3′ 5′-CCTCCTCTCCGAAATCCTCT-3′
Glyceraldehyde-3-phosphate dehydrogenase	Forward Reverse	5′-CGG TGC TGA GTA TGT CGT GGA-3′ 5′-GGC AGA AGG GGC GGA GAT GA-3′
Facilitated glucose transporter 2	Forward Reverse	5′-GCACAGACACCCCACTTACA-3′ 5′-CACCCACCAAAGAATGAGG-3′
Thrombospondin 4	Forward Reverse	5′-CGACTTGGTGTGTTCTGCTT-3′ 5′-GTTGTGGGATTGCTTCTTGG-3′
Farnesyl pyrophosphate synthetase	Forward Reverse	5′-GAGCAGACACTGAACCACCA-3′ 5′-ATTGATGCGGAGAAGGAACA-3′
RhoC	Forward Reverse	5′-CCCTTCCTCCCTGCCTCT-3′ 5′-CAGAAACCCCAGTCCCTACC-3′
Rho-associated, coiled-coil forming protein kinase p160 (Rock1)	Forward Reverse	5′-TCAGATTGTTTGCTGGATGG-3′ 5′-TGCCGATTACCTTTACCACTT-3′
Tissue inhibitor of metalloproteinase 3	Forward Reverse	5′-ACTCTTCCCTGCCTCACATC-3′ 5′-TCCTGCCTTCTCCCATTTC-3′
Neurophilin 1	Forward Reverse	5′-TGCGGTAACAACAGGAATCA-3′ 5′-CCACAGGGTAAGGAGAAAGAGA-3′
Vascular endothelial growth factor receptor 2 (Flk-1)	Forward Reverse	5′-GTGGACTGGGAGGAAGGAAG-3′ 5′-GACTGTGAAGAGCACGCAAA-3′
Vascular endothelial growth factor receptor 1 (Flt-1)	Forward Reverse	5′-TATAAGGCAGCGGATTGACC-3′ 5′-TCATACACATGCACGGAGGT-3′
Angiotensinogen	Forward Reverse	5′-CTGACCCAGTTCTTGCCACT-3′ 5′-CACCGAGATGCTGTTGTCC-3′
Vascular endothelial growth factor A	Forward Reverse	5′-CACGACAGAAGGAGAGCAGA-3′ 5′-ATCAGCGGCACACAGGAC-3′
Vascular endothelial growth factor B	Forward Reverse	5′-ACAGGGAGAAGAGTGGAGCA-3′ 5′-TGGTAGAAGTTTGGGGTTTT-3′
Vascular endothelial growth factor C	Forward Reverse	5′-GGAAATGTGCCTGTGAATGT-3′ 5′-GACTGTGACTGACTGAAAACT-3′
CD151	Forward Reverse	5′-GGTGGCTGGTGTTGTTGTC-3′ 5′-GCCTGACTGGTGGTATCTCTT-3′
RAC3	Forward Reverse	5′-ACCCATAACCTACCCCCAAG-3′ 5′-CAGCAGACTCAGGGACATCA-3′
Calcineurin	Forward Reverse	5′-CGGAAGGAAGTCATCAGAAA-3′ 5′-CAGCCTCAATAGCCTCAACA-3′
Angiopoietin 2	Forward Reverse	5′-CAAGGCACTGAGAGACACCA-3′ 5′-CTGAACTCCCACGGAACATT-3′
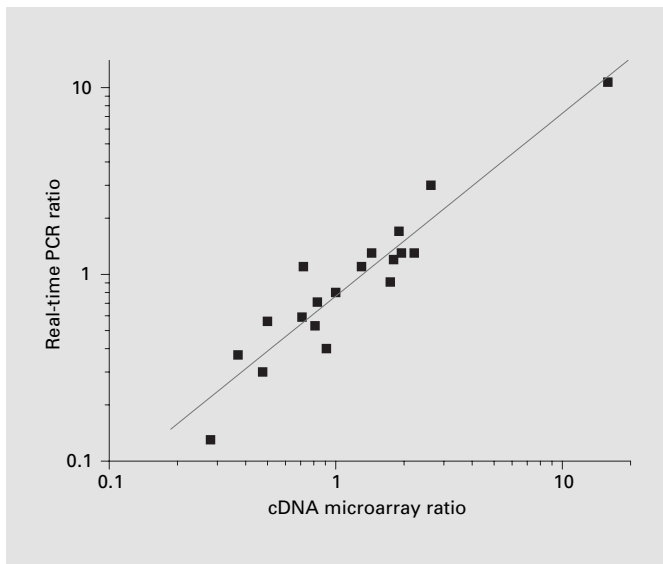
Fig. 1. Confirmation of cDNA microarray results with real-time PCR. To technically verify the cDNA microarray results, the expression of 19 randomly selected up-regulated, down-regulated and unaffected genes were quantified by real-time PCR using the amplified RNA that was used for the microarray experiments. The graph illustrates the correlation (0.98) between the fold regulation in RT[NC/KO] versus RT islets measured by cDNA microarray and real-time PCR.

Fisher's exact test was applied to test for significant difference between the observed number and the expected number.

Quantitative Real-Time PCR
One microgram amplified aRNA was mixed with 4 μl random hexamers (0.5 μg/μl; Promega, UK) and reverse transcribed and real-time PCR amplified as described [6]. The optimal running concentration of $MgCl_2$, dNTP and primers were found by Evolutionary Operation [7]. Primer sequences are listed in table 1. The correct real-time PCR product was confirmed by melting curve analysis and agarose gel electrophoresis (2% w/v). Quantification strategy and data analysis of the relative gene expression between RT and RT[NC/KO] were done as described [8, 9]. Expression data were normalized against acidic ribosomal phosphoprotein PO.

Immunoreagents
Antibodies used for immunostainings include rabbit anti-collagen IV (1:250; Biogenesis), rabbit anti-fibronectin (1:200; Dako A/S Denmark), monoclonal anti-vinculin (1:50; Sigma), mouse monoclonal anti-laminin $α_1$ (generous gift from Dr. P. Ekblom), rat anti-$β_1$-integrin (9EG7; 1:500; Becton Dickson), rabbit anti-$β_1$-integrin (generous gift from Dr. S. Johansson), biotin-conjugated donkey anti-rabbit (1:1,000; Jackson ImmunoResearch), biotin-conjugated donkey anti-rat (1:750; Jackson ImmunoResearch), Cy3-conjugated goat anti-rat (1:100; Jackson ImmunoResearch). Cy3-conjugated streptavidin (1:1,500; Jackson ImmunoResearch) were used for visualizing secondary antibodies. Antibodies used for immunoblotting include goat anti-$β_1$-integrin (1:200; Santa Cruz Biotechnology), biotin-

conjugated anti-goat (1:500; Dako A/S Denmark), streptavidin-HRP (1:2,000; Dako A/S Denmark).

Immunohistochemistry
Cryosections (8 μm) of paraformaldehyde-fixed tissues were incubated with primary antibodies diluted in PBS supplemented with 5% skim milk at 4°C overnight. Secondary antibodies and streptavidin-alexa 633 were incubated at room temperature for 1 h. The fact that vinculin cannot be located on tissue sections led us to examine vinculin in primary tumour cells. Primary tumour cells were isolated from late-stage (13–14 weeks) RT and RT[NC/KO] tumours, plated on polylysine-treated cover slips, fixed with 4% PFA and stained according to the immunofluorescence staining procedure as described above.

Tumour Cell Adhesion Assay
Tumour cells were dissected from 13- to 14-week-old RT and RT[NC/KO] tumours. Cells were suspended in culture medium (Dulbecco's modified Eagle's medium supplemented with 10% fetal calf serum, 100 U/ml penicillin and 100 μg/ml L-glutamate) and counted in a Bürcher chamber. Cell adhesion assay was performed as previously described [4].

Results

Gene Expression Changes Associated with N-CAM-Deficient β Tumour Cell Progression

To further resolve by which mechanism N-CAM limits tumour cell disaggregation and metastasis during RT tumour progression, we compared the gene expression pattern in RT and RT[NC/KO] β tumour cells. To avoid secondary gene expression changes due to tissue disaggregation and tumour cell necrosis, we chose to focus on events taking place early during tumour progression (8 weeks). RNA was isolated from pancreatic islets of 8-week-old RT and RT[NC/KO] mice. The RNA was amplified and compared on cDNA microarray chips containing 5,501 different genes. Only 1.5-fold or greater changes were considered. Among 5,501 genes, 401 and 296 genes were up-regulated and down-regulated, respectively (for a full list of the regulated genes, see supplementary data).

To technically verify the cDNA microarray results, the expression of 19 randomly selected up-regulated, down-regulated and unaffected genes were quantified by real-time PCR using the amplified RNA that was used for the microarray experiments. The concurrence of the microarray or real-time PCR results shows that the microarray results were technically reproducible (fig. 1).

The regulated genes were classified into different categories by using Gene Ontology terms (table 2). Many genes related to cell adhesion (cell adhesion, cell-matrix adhesion), cell motility (cell adhesion, cell-matrix adhe-

Håkansson/Xian/He/Ståhlberg/Nelander/
Samuelsson/Kubista/Semb

Table 2. Groups of regulated genes

Gene ontology term/gene name	Regulation ($RT^{NC/KO}/RT$)[1]	Gene ontology term/gene name	Regulation ($RT^{NC/KO}/RT$)[1]
Cell adhesion		*Ras- and Rho-related genes*	
Leucine-rich repeat protein 1, neuronal	1.8	Ras homolog gene family, member C	1.9
Cadherin 1	1.6	Ras-like protein	−1.6
Flotillin 1	1.6	RAC2	−1.6
Laminin γ_1	1.6	Ras homolog gene family, member J	−1.6
Collagen α_1 (III) chain	−1.5	Destrin	−1.9
Procollagen, type VIII, α_1	−1.5	Kinesin-associated protein 3	−2.0
Flotillin 2	−1.6	Rho-associated coiled-coil forming kinase 1	−2.7
Catenin src	−1.6	RAS-related protein 1a	−1.8
RIKEN cDNA 9430041O17 gene	−1.7	V-crk sarcoma virus CT10 oncogene homolog	
Biglycan	−1.8	(avian)	−1.9
Collagen α_3 (VI) chain	−1.9	*Actin cytoskeleton*	
Lectin, galactose binding, soluble 9	−2.1	Actinin α_3	2.3
Vinculin	−2.3	RIKEN cDNA 0610025L06 gene	1.6
Fibronectin	−2.8	CD2-associated protein	−1.6
Vascular cell adhesion molecule 1	−2.8	Septin 2	−1.6
Cell-matrix adhesion		RIKEN cDNA 9430041O17 gene	−1.7
Integrin α_6	−1.6	Striamin	−1.7
RIKEN cDNA 9430041O17 gene	−1.7	ARP2/3 complex 34 kDa subunit-related	−1.7
Fibulin 2	−2.2	Myosin IIIA	−1.7
Thrombospondin 4	−4.3	Calcium/calmodulin-dependent protein kinase II, δ	−1.8
ECM		Destrin	−1.9
Laminin γ_1	1.6	Myosin-binding subunit of myosin phosphatase-	
Procollagen, type VIII, α_1	−1.5	related	−2.1
MMP 2	−1.5	Palladin	−2.1
Biglycan	−1.8	Radixin	−2.6
Collagen α_3 (VI) chain	−1.9	Rho-associated coiled-coil forming kinase 1	−2.7
Similar to microfibril-associated genes		*Actin cytoskeleton reorganization*	
Glycoprotein 3 precursor	−1.9	Ras homolog gene family, member C	1.9
Secreted acidic cysteine-rich glycoprotein	−2.0	Ras-like protein	−1.6
Tissue inhibitor of metalloproteinase 2	−2.0	RAC2	−1.6
Tissue inhibitor of metalloproteinase 3	−2.0	Ras homolog gene family, member J	−1.6
Fibulin 2	−2.2	Brefeldin A-inhibited guanine nucleotide exchange	
Elastin	−2.2	protein	−1.6
Fibronectin	−2.8	Destrin	−1.9
Thrombospondin 4	−4.3	Rho-associated coiled-coil forming kinase 1	−2.7
Collagen binding		Tumor antigen	
Collagen α_1 (III) chain	−1.5	Kangai 1 (suppression of tumorigenicity 6, prostate)	2.6
Cerebellin related	−1.5	Folate receptor 1 (adult)	1.8
Integrin α_6	−1.6	Melanoma antigen, family D, 2	1.9
		RIKEN cDNA 2010107K23 gene	1.7
		Squamous cell carcinoma antigen recognized by	
		T cells 1	1.6

[1]   The ratios were calculated as the expression level from $RT^{NC/KO}$ divided by the expression level from RT. If the value was <1, the value was inverted and prefixed with a '−' sign indicating a negative fold regulation.
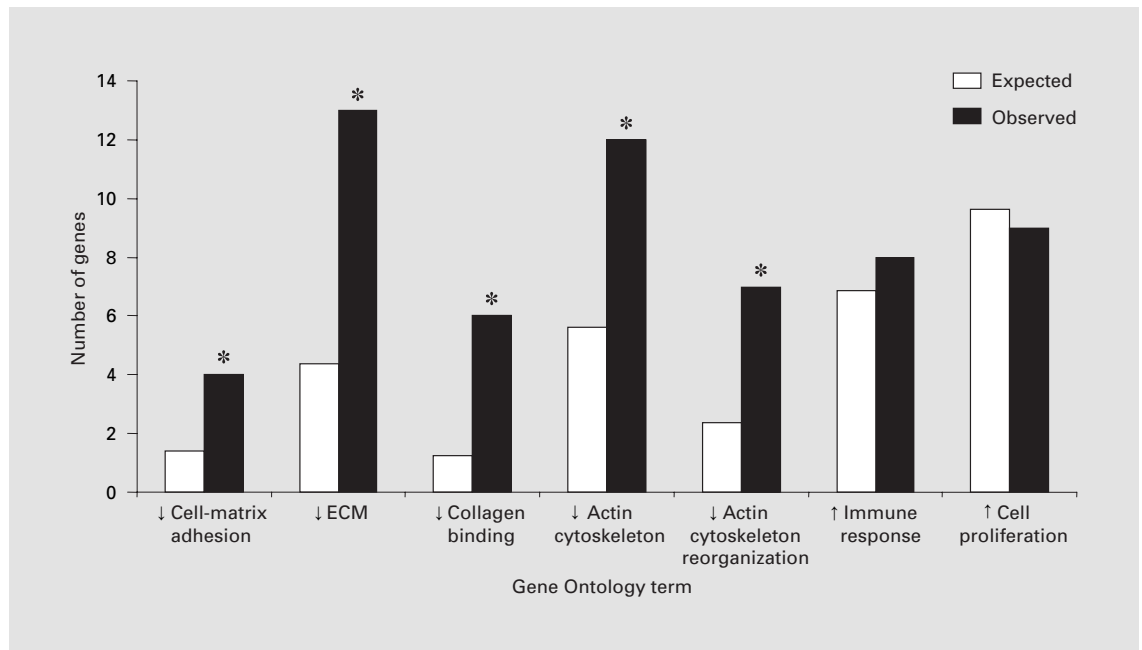
Fig. 2. Extent of gene expression changes within gene groups. The number of regulated genes in each group (■) is compared with the expected number (□). The gene groups with the Gene Ontology term cell-matrix adhesion, ECM, collagen binding, actin cytoskeleton and actin cytoskeleton reorganization were significantly regulated, whereas immune response and cell proliferation genes were not. ↓ = Down-regulated genes; ↑ = up-regulated genes; * = $p < 0.05$. The statistical method used was Fisher's exact test.

sion, ECM, Rho GTPases, actin cytoskeleton dynamics) and tumour cell antigens were regulated, and for several of these categories, most genes were regulated in a coordinated manner (table 2, fig. 2).

The most coherently regulated gene category was ECM molecules. The predicted outcome of these gene expression changes during RT[NC/KO] tumour progression is the diminished production of ECM molecules, such as collagen III, VI and VIII, fibronectin, secreted acidic cysteine-rich glycoprotein, elastin, thrombospondin 4, laminin α_1 (2-fold average down-regulation in three experiments, whereas one experiment showed no effect, data not shown) and of cell matrix-adhesion constituents, such as α_6-integrin and vinculin (table 2).

In contrast to cell-matrix adhesion, no consistent regulation of tumour cell-cell adhesion molecules was observed. However, changes that were observed included a slight up-regulation of cadherin 1 and a down-regulation of vascular cell adhesion molecule 1 (table 2) that is mainly expressed by endothelial cells [10].

Defective ECM Deposition in the Tumour Cell Stroma during N-CAM-Deficient β Tumour Cell Progression

Histopathological analysis demonstrated tissue disaggregation at late stages of tumour development in RT[NC/KO] mice [4] (fig. 3), suggesting defects in cell-cell and/or cell-matrix adhesion. The fact that cadherin-mediated cell-cell adhesion appears unaffected in RT[NC/KO] mice [3] suggested that N-CAM-deficient β tumour cells may display cell-matrix adhesion defects in vivo. Indeed, when we examined the deposition of major ECM stromal components, such as fibronectin, laminin 1 and collagen IV, at late stages of tumour progression when the tumour tissue disaggregation is apparent (12–14 weeks), all three ECM components were affected. Normally, these ECM molecules are distributed in continuous sheets within the stroma, with a somewhat more focal concentration of laminin 1 (fig. 4A, D, G). Collagen IV was basically unaffected in areas of intact RT[NC/KO] tumour tissue (fig. 4B), whereas less collagen IV was deposited in a discontinuous fashion within areas of disaggregated tumour tissue (fig. 4C). Changes in the deposition of fibronectin and laminin 1 were more extensive as they were observed both
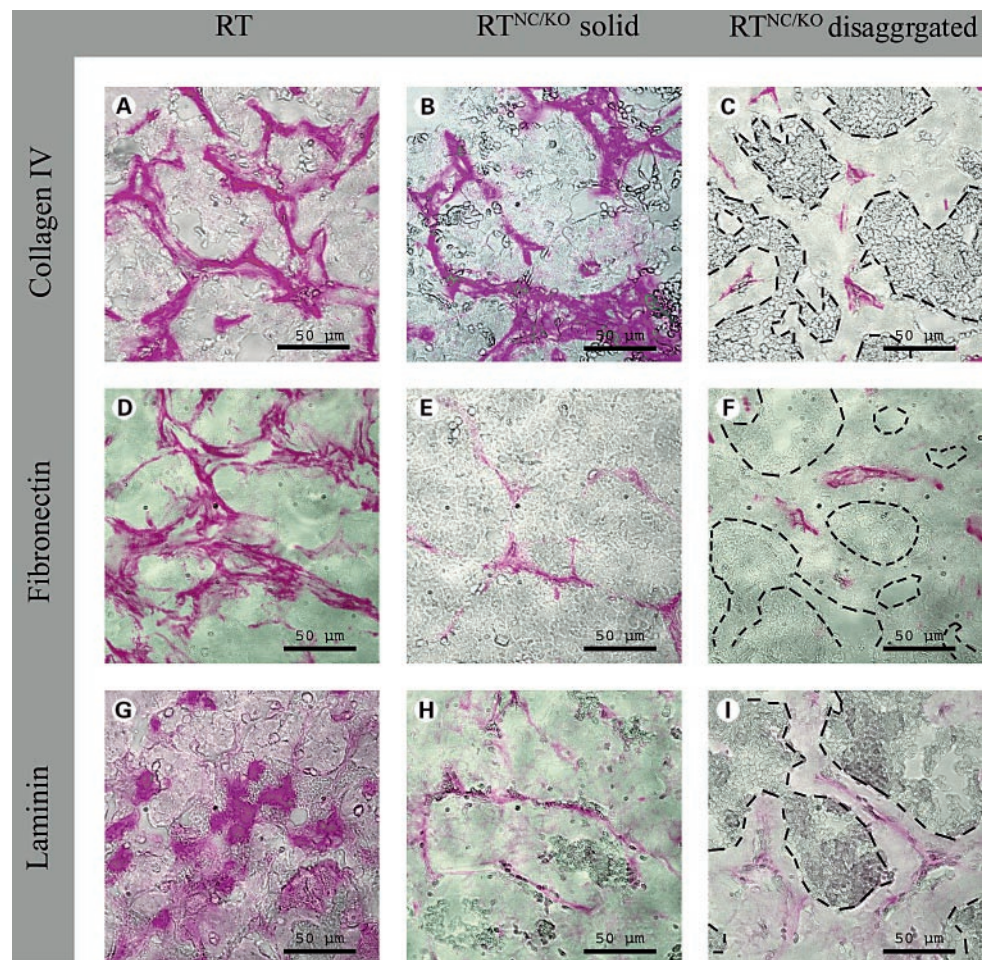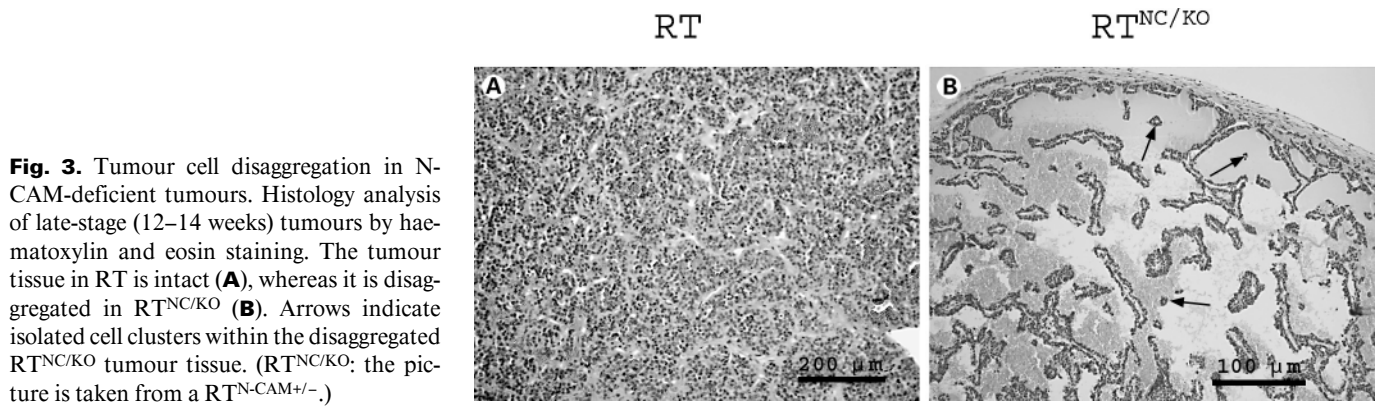
Håkansson/Xian/He/Ståhlberg/Nelander/
Samuelsson/Kubista/Semb

Fig. 3. Tumour cell disaggregation in N-CAM-deficient tumours. Histology analysis of late-stage (12–14 weeks) tumours by haematoxylin and eosin staining. The tumour tissue in RT is intact (**A**), whereas it is disaggregated in RT^NC/KO (**B**). Arrows indicate isolated cell clusters within the disaggregated RT^NC/KO tumour tissue. (RT^NC/KO: the picture is taken from a RT^N-CAM+/−.)

Fig. 4. N-CAM-induced cell disaggregation is accompanied by changes in the deposition of ECM components. Consecutive sections of 14-week-old RT and RT^NC/KO tumours were stained with antibodies against collagen IV (**A**, **B**, **C**), fibronectin (**D**, **E**, **F**) and laminin α1 (**G**, **H**, **I**) (purple). All ECM components were distributed in continuous sheets in RT tumours, with a somewhat more focally concentrated distribution of laminin 1. Whereas collagen IV was unaffected in RT^NC/KO solid tumour tissue (**B**), the deposition of both fibronectin and laminin 1 was decreased (**E**, **H**). However, all three ECM components were deposited at much lower levels in a discontinuous manner in disaggregated areas of RT^NC/KO tumours (**C**, **F**, **I**). All images are overlays of phase contrast and staining images. Blood-filled cavities not apparent by morphology are indicated by dotted lines. (RT^NC/KO: the pictures are taken from RT^N-CAM+/−.)
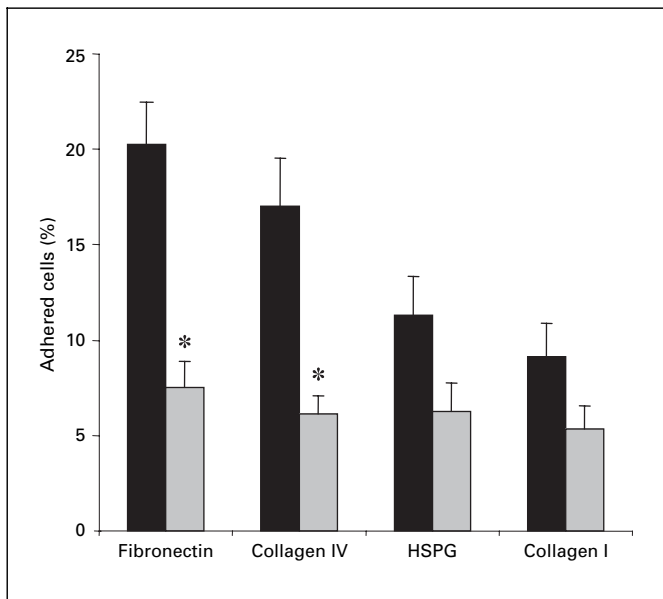
Fig. 5. N-CAM deficiency results in decreased adhesion of β tumour cells to fibronectin and collagen IV. Tumour cells from tumours of 13- to 14-week-old RT and RT$^{NC/KO}$ mice were seeded on plates coated with fibronectin, HSPG, collagen IV and collagen I. Adhesion of RT$^{NC/KO}$ cells to fibronectin and collagen IV was significantly inhibited (n = 9, both for RT and RT$^{NC/KO}$). * = p < 0.001. p for HSPG and collagen I adhesion was 0.06 and 0.09, respectively. The statistical method used was Student's t test.

Fig. 6. N-CAM deficiency results in decreased vinculin expression but no change in β$_1$-integrin. Western blot shows no regulation in the general form of β$_1$-integrin (**A**). Expression of the active form of β$_1$-integrin, which is detected by immunostaining, showed no difference between RT and RT$^{NC/KO}$ tumours (**B**, **C**). The active β$_1$-integrin is expressed both in endothelial and β tumour cells. Expression of vinculin was down-regulated in RT$^{NC/KO}$ primary tumour cells (**E**) compared with RT tumour cells (**D**). (RT$^{NC/KO}$: the picture is taken from a RT$^{N-CAM+/-}$.)

in intact and disaggregated tumour tissue, suggesting that the changes were not secondary to tissue disaggregation. However, the changes were qualitatively similar to collagen IV, i.e. deposition of less protein in a discontinuous pattern (fig. 4E, F, H, I).

In addition to diminished ECM deposition, perturbed tumour cell-matrix adhesion could contribute to the observed tumour cell disaggregation. Therefore, cell-matrix adhesion assays were performed on primary tumour cells dissected from late-stage (13–14 weeks) RT and RT$^{NC/KO}$ tumours. The results indicate a general cell-matrix adhesion deficiency towards the studied matrix components, i.e. collagen I, collagen IV, heparansulphate proteoglycan (HSPG) and fibronectin. However, significantly impaired matrix adhesion was only observed to collagen IV and fibronectin (fig. 5).

The fact that β$_1$-integrin is the major receptor for collagen IV and fibronectin suggested that the observed changes in matrix adhesion could be explained by changes in the expression and/or activation of β$_1$-integrin. However, neither the expression level nor the activation status
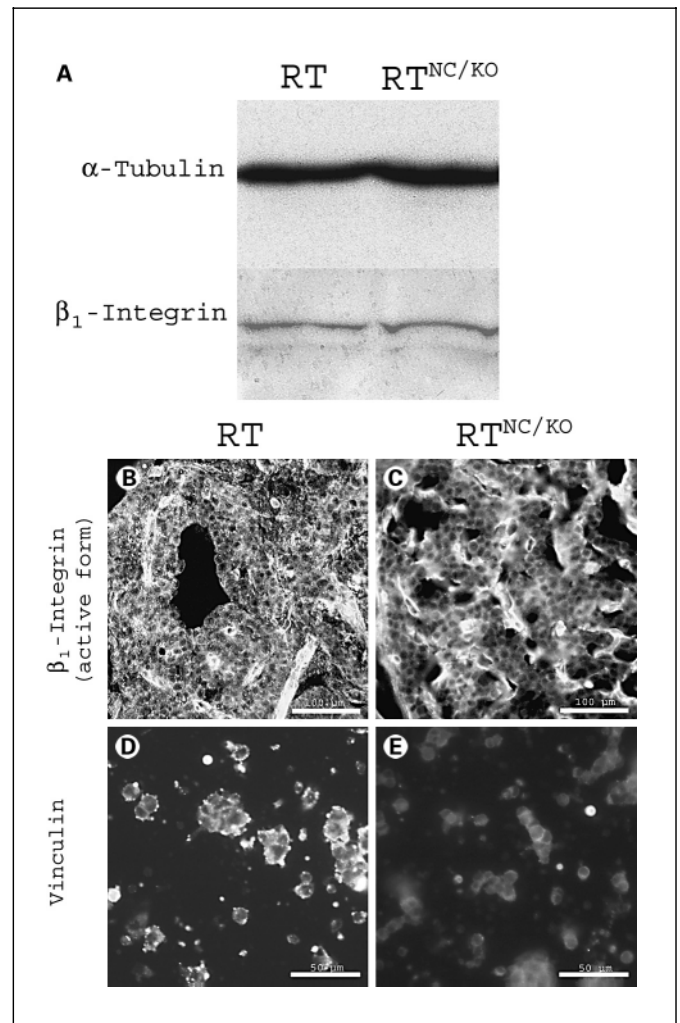
of β$_1$-integrin appeared to be affected in N-CAM-deficient tumour cells (fig. 6A–C). Interestingly, vinculin, which mediates contacts between integrins and the actin cytoskeleton, was down-regulated in RT$^{NC/KO}$ tumour cells (table 2, fig. 6D, E), suggesting a potential mechanism for defective tumour cell-matrix adhesion.

Håkansson/Xian/He/Ståhlberg/Nelander/
Samuelsson/Kubista/Semb

Discussion

Here, we report gene expression changes associated with N-CAM-deficient β tumour cell dissemination. The regulated genes belong to different categories representing various aspects of cell behaviour, such as cell adhesion and cell migration, which are known effectors of tumour cell progression. In particular, N-CAM ablation during β tumour cell progression resulted in an overall diminished expression of ECM molecules and of components necessary for cell-matrix adhesion. Indeed, this finding correlated with deficient deposition of ECM components in the tumour cell stroma and perturbed tumour cell-matrix adhesion. All together, these findings demonstrate that N-CAM is necessary for maintaining normal deposition of ECM molecules within the tumour cell stroma and for tumour cell-matrix adhesion during β cell carcinogenesis, implying a potential mechanism for N-CAM's role in limiting β tumour cell dissemination. However, to conclude whether the effects on ECM production and tumour cell-matrix adhesion are causally involved in N-CAM-deficient β tumour cell metastasis requires further investigations.

Potential Roles of N-CAM in β Tumour Cell Disaggregation

During malignancy, increased dissociation of tumour cells from the primary tumour by changes in cell-cell adhesion and cell-matrix adhesion contributes to tumour cell dissemination. Consequently, the increased tumour cell dissociation associated with N-CAM-deficient β tumour cell progression may be mechanistically involved in β tumour cell metastasis.

Notably, we show that N-CAM deficiency during β tumour cell progression results in a general down-regulated expression of ECM molecules. Not only were the major ECM components like fibronectin and collagens down-regulated, but also α_6-integrin and the focal adhesion protein vinculin, which together with other adaptor proteins mediates contacts between integrins and the actin cytoskeleton. Interestingly, a potential consequence of the reduced expression of ECM molecules was the apparent deficient incorporation of ECM molecules in the tumour cell stroma.

Additionally, cell-matrix adhesion assays revealed an overall disturbed tumour cell-matrix interaction. Although the adhesion towards all of the tested matrix components appeared disturbed, only adhesion to collagen IV and fibronectin was significantly lowered. These results are partially in agreement with recent studies on RT[NC/KO]

tumour cell lines in that they exhibit significantly impaired adhesion to collagen IV. However, in contrast to our results, the RT[NC/KO] tumour cell lines also exhibited impaired adhesion to HSPG, but not to fibronectin [4]. The fact that no apparent effects in the expression or activation of β_1-integrin was detected does not rule out changes in the activation status of a particular α/β_1 heterodimer since the anti-β_1-integrin antibodies recognize all forms of β_1-integrin [11].

In summary, the defective ECM production/deposition and/or tumour cell-matrix adhesion may represent the underlying cause for tumour tissue disaggregation induced by N-CAM ablation. These events may secondarily contribute to the metastatic spreading of β tumour cells.

Does N-CAM Influence β Tumour Cell Migration?

Tumour cell dissociation per se is most likely not sufficient for inducing tumour cell metastasis. Activation of tumour cell migration is probably also necessary since increased cell migration is considered to be intimately associated with tumour cell invasion and metastasis [12]. Consequently, N-CAM's limiting role in β tumour cell dissemination suggests that N-CAM deficiency could be associated with increased cell migration.

To migrate, cells are driven by the force of extending protrusions or lamellipodia, setting up new adhesion sites at the front, contracting the cell body and detaching from the adhesion site at the cell rear [13]. The whole process involves disrupting and building up cell adhesion, ECM degradation, remodelling and the reorganization of the actin cytoskeleton. Matrix metalloproteinases (MMPs) are known to contribute to cell migration by degrading the matrix proteins [14]. Interestingly, the inhibitors of MMPs, tissue inhibitor of metalloproteinase 2 and 3 (table 2) were both down-regulated in RT[NC/KO], implicating an increased MMP activity. However, we detected no difference in the overall activity of MMPs between RT and RT[NC/KO] angiogenic islets (data not shown). This finding, however, does not exclude the possibility that individual islets may exhibit locally increased activity of MMPs.

In summary, although reduced expression and deposition of ECM components may create a microenvironment which is easier for tumour cells to penetrate, complimentary experimental strategies are needed to more specifically address N-CAM's influence on cell migration during β tumour cell progression.

Acknowledgements

References

1 Cavallaro U, Christofori G: Cell adhesion in tumor invasion and metastasis: Loss of the glue is not enough. Biochim Biophys Acta 2001; 1552:39–45.

2 Hanahan D: Heritable formation of pancreatic beta-cell tumours in transgenic mice expressing recombinant insulin/simian virus 40 oncogenes. Nature 1985;315:115–122.

3 Perl AK, Dahl U, Wilgenbus P, Cremer H, Semb H, Christofori G: Reduced expression of neural cell adhesion molecule induces metastatic dissemination of pancreatic beta tumor cells. Nat Med 1999;5:286–291.

4 Cavallaro U, Niedermeyer J, Fuxa M, Christofori G: N-CAM modulates tumour-cell adhesion to matrix by inducing FGF-receptor signalling. Nat Cell Biol 2001;3:650–657.

5 Scheidl SJ, Nilsson S, Kalen M, et al: mRNA expression profiling of laser microbeam microdissected cells from slender embryonic structures. Am J Pathol 2002;160:801–813.

6 Stahlberg A, Hakansson J, Xian X, Semb H, Kubista M: Properties of the reverse transcription reaction in mRNA quantification. Clin Chem 2004;50:509–515.

7 Montgomery DC: Design and Analysis of Experiments, ed 4. New York, John Wiley & Sons, 1997, pp 616–622.

8 Stahlberg A, Aman P, Ridell B, Mostad P, Kubista M: Quantitative real-time PCR method for detection of B-lymphocyte monoclonality by comparison of kappa and lambda immunoglobulin light chain expression. Clin Chem 2003;49:51–59.

9 Pfaffl MW: A new mathematical model for relative quantification in real-time RT-PCR. Nucleic Acids Res 2001;29:e45.

10 Osborn L, Hession C, Tizard R, et al: Direct expression cloning of vascular cell adhesion molecule 1, a cytokine-induced endothelial protein that binds to lymphocytes. Cell 1989; 59:1203–1211.

11 Bottger BA, Hedin U, Johansson S, Thyberg J: Integrin-type fibronectin receptors of rat arterial smooth muscle cells: Isolation, partial characterization and role in cytoskeletal organization and control of differentiated properties. Differentiation 1989;41:158–167.

12 Thiery JP: Epithelial-mesenchymal transitions in tumour progression. Nat Rev Cancer 2002; 2:442–454.

13 Raftopoulou M, Hall A: Cell migration: Rho GTPases lead the way. Dev Biol 2004;265:23–32.

14 Egeblad M, Werb Z: New functions for the matrix metalloproteinases in cancer progression. Nat Rev Cancer 2002;2:161–174.